JCB Article

Integrins engage mitochondrial function for signal transduction by a mechanism dependent on Rho GTPases

Erica Werner and Zena Werb

Department of Anatomy, University of California, San Francisco, CA 94143

We show here the transient activation of the small GTPase Rac, followed by a rise in reactive oxygen species (ROS), as necessary early steps in a signal transduction cascade that lead to NFκB activation and collagenase-1 (CL-1)/matrix metalloproteinase-1 production after integrin-mediated cell shape changes. We show evidence indicating that this constitutes a new mechanism for ROS production mediated by small GTPases. Activated RhoA also induced ROS production and up-regulated CL-1 expression. A Rac mutant (L37) that prevents reorganization of the actin cytoskeleton prevented integrin-induced CL-1 expression, whereas mutations that abrogate Rac binding to the neutrophil NADPH membrane oxidase in vitro (H26 and N130) did not. Instead, ROS were produced by integrin-induced changes in mitochondrial function, which were inhibited by Bcl-2 and involved transient membrane potential loss. The cells showing this transient decrease in mitochondrial membrane potential were already committed to CL-1 expression. These results unveil a new molecular mechanism of signal transduction triggered by integrin engagement where a global mitochondrial metabolic response leads to gene expression rather than apoptosis.

Introduction

Reactive oxygen species (ROS)* are intermediaries in signal transduction cascades regulating cell proliferation, differentiation, and death (for reviews see Thannickal and Fanburg, 2000; Droge, 2002). A prooxidant state may promote proliferation (Huang et al., 2000), and the expression of an exogenous oxidase induces cell transformation (Suh et al., 1999), whereas diminution of intracellular ROS levels by overexpression of manganese superoxide dismutase inhibits proliferation (Li et al., 1998). ROS are also involved in cell differentiation. During PC12 differentiation, NGF-induced ROS production is required for neurite outgrowth (Suzukawa et al., 2000). The intracellular redox status influences the balance of self-renewal and differentiation of glial precursor cells (Smith et al., 2000). ROS are also induced during cell stress, cell death, and senescence (Lee et al., 1999). The participation of ROS in such diverse cellular processes suggests a tight control for their production and function.

In most of these pathways, the mechanisms for ROS production and their molecular targets remain largely unknown. At least three distinct mechanisms have been identified: upon neutrophil activation, superoxide is produced in the phagosome by a membrane oxidase to kill the endocytosed pathogen. In nonphagocytic cells, a different mechanism is used in association with activation of EGF (Bae et al., 1997) and PDGF receptors (Sundaresan et al., 1995). In these systems, ROS are produced by a distinct oxidase at the plasma membrane, inhibiting phosphatases and potentiating tyrosine kinases signaling (Lee et al., 1998; Barrett et al., 1999).

Mitochondria are the third and most important source for ROS in every cell type, where 1–5% of the transported electrons is diverted to the formation of superoxide instead of water (Boveris et al., 1972). Although the molecular mechanisms involved in the mitochondrial switch to ROS production are not well understood, multiple pathways may converge to modify mitochondrial function. Moreover, recent studies also indicate that the production of ROS may be accompanied by changes in mitochondrial metabolism (Nemoto et al., 2000; Nicholls and Budd, 2000). The rate of mitochondrial superoxide production is modulated during TNFα signaling (Schulze-Osthoff et al.,

Address correspondence to Erica Werner, Dept. of Cell Biology, Emory University, Whitehead Biomedical Research Bldg., 615 Michael St., Atlanta, GA 30322. Tel.: (404) 727-6277. Fax: (404) 727-6456.
E-mail: ericaw@cellbio.emory.edu

E. Werner's present address is Dept. of Cell Biology, Emory University, Whitehead Biomedical Research Bldg., 615 Michael St., Atlanta, GA 30322.

*Abbreviations used in this paper: CL-1, collagenase-1; LH, lactalbumin hydrolysate; mAb, monoclonal antibody; MMP, matrix metalloproteinase; MPT, membrane permeability transition; MTT, dimethylthiazolyldiphenyltetrazolium bromide; NBT, nitroblue tetrazolium; ROS, reactive oxygen species; RSF, rabbit synovial fibroblast.

Key words: integrin; actin; Rac; ROS; mitochondria

1993; Sanchez-Alcazar et al., 2000), hypoxia (Vanden Hoek et al., 1997; Chandel et al., 1998), and apoptosis (Cai and Jones, 1998).

The small GTPase Rac has emerged as a common mediator of ROS production in diverse signaling pathways that lead to mitogenesis, gene expression, and stress responses (Irani et al., 1997; Page et al., 1999; Ozaki et al., 2000; Suzukawa et al., 2000). The molecular mechanisms involved have been identified through the use of mutations in Rac that modify its interaction with effector proteins. The best understood mechanism is promotion of ROS production in neutrophils where Rac2 binds to a NAD(P)H oxidase through the insertion domain and residue 26 in the effector domain to mediate assembly and function of the burst oxidase at the plasma membrane (Freeman et al., 1996). In most other cell types, the oxidase remains unidentified. In Ras-induced NIH 3T3 cell transformation, Rac1 is necessary and sufficient to induce ROS production by a mechanism dependent on the insertion domain (residues 124–135) (Irani et al., 1997; Joneson and Bar-Sagi, 1998). However, there are other pathways where Rac promotes ROS production by a distinct mechanism. During PDGF-induced cyclin D expression, Rac-mediated ROS production depends on the residues 33 and 37 of the effector domain (Joyce et al., 1999; Page et al., 1999). Rac mediates ROS production during noncytotoxic TNFα signaling by an indirect mechanism involving phospholipase A2 (Woo et al., 2000). These observations suggest that Rac may act at different steps to control ROS production.

In rabbit synovial fibroblasts (RSFs), clustering of integrins by anti-α5 integrin antibodies leads to altered adhesion followed by the reorganization of the actin cytoskeleton and the production of ROS. As a result, the transcription factor NFκB is activated, inducing the expression of IL-1 and matrix metalloproteinase (MMP)-1/collagenase-1 (CL-1) (Kheradmand et al., 1998). In the present study, we have elucidated the pathway by which integrin-mediated signaling induces ROS production.

Results

Integrin ligation activates Rac upstream from ROS and CL-1 induction

We have observed previously that integrin-dependent cell shape changes in RSFs induce CL-1 gene expression through a Rac- and ROS-dependent mechanism (Kheradmand et al., 1998). The antioxidants Tiron (1,2-dihidroxybenzene-3,5-disulphonic acid; a superoxide scavenger) or catalase prevented CL-1 induced by anti-α5 monoclonal antibody (mAb; a fibronectin receptor function-perturbing antibody BIIG2) (Fig. 1 A). To measure whether soluble anti-α5 mAb increases endogenous ROS production, we used H_2O_2-driven peroxidase oxidation of homovanillic acid into a fluorogenic product. This assay allows the analysis of ROS production in the extracellular medium without compromising cell integrity or shape. Intracellular superoxide ions are rapidly transformed by superoxide dismutases into H_2O_2, a more stable and membrane-permeable species, which diffuses in the cytosol and to the extracellular fluid. Upon addition of anti-α5 mAb, we detected a transient increase in H_2O_2, which peaked at 120 min (Fig. 1 B).

Our previous experiments with overexpression of GTPase function-altering mutants suggested a role for Rac in anti-α5 mAb–induced H_2O_2 and CL-1 production. To demonstrate whether endogenous Rac is activated during integrin-induced cell shape change, we prepared cell lysates from cultures treated with anti-α5 mAb for different intervals. Activated Rac was isolated from the cell lysates using the recombinant Rac-binding domain of PAK bound to agarose beads (Benard et al., 1999) and detected with anti-Rac antibodies by Western blot analysis of the precipitates. As a control, GTP or GDP was directly added to lysates. After integrin activation, Rac–GTP levels increased transiently peaking between 30 and 60 min (Fig. 1 C). Densitometric analysis evidenced a 2.8-old increase in the levels of Rac activity, which returned to basal levels after 60 min. Careful comparison of the kinetics of Rac activation with the timing of ROS production, showed that Rac activation (Fig. 1 C) precedes the rise in ROS production (Fig. 1 B), which peaks 2 h after addition of anti-α5 mAb. Rac is necessary for the integrin-dependent increase in H_2O_2 production because a dominant interfering Rac mutant (RacN17) prevented the rise in H_2O_2 (unpublished data) as we found previously (Kheradmand et al., 1998). Moreover, activated Rac is sufficient for H_2O_2 production because expression of an activated mutant, RacV12, induced both a rise in H_2O_2 and the downstream induction of CL-1 (Fig. 1 D). Other members of the Rho GTPase family also mediate integrin-dependent signaling (Werner et al., 2001) and cytoskeletal reorganization (Nobes and Hall, 1995; Caron and Hall, 1998). We found that activation of Rac was not unique in its ability to induce a H_2O_2 rise and CL-1 expression. Constitutively activated Rho (RhoA V14) (Fig. 1 D) but not constitutively activated Cdc42 V12 (unpublished data) was also effective in inducing H_2O_2 and CL-1 production. This experiment shows that ROS induction is not restricted as a downstream consequence of Rac activation but is triggered by RhoA.

To gain insights into the mechanism used by GTPases to trigger an increase in ROS production and induce CL-1 expression, we used point mutations that selectively disrupt effector domain functions of the constitutively active mutants RacV12 and RacL61 (Westwick et al., 1997). When we cotransfected RSFs with a panel of different Rac effector domain point mutants together with a CL-1 promoter reporter construct, we observed that only the mutant L37 was completely unable to induce expression of a CL-1 (Fig. 2 A) or NFκB (Fig. 2 B) promoter–reporter constructs. We compared the RacV12 H26 mutant in the switch 1 effector domain with the RacV12 N130 mutant in the insertion domain, both of which can activate other Rac effectors, such as PAK, but cannot activate the neutrophil oxidase in vitro (Freeman et al., 1996). In contrast to the L37 mutant, neither mutant was impaired in the induction of the expression of the NFκB promoter, a step in the pathway more proximal to the integrin signal than CL-1 expression (Fig. 2 B), or of the CL-1 promoter (unpublished data). These results suggest that Rac activates a signaling pathway by an effector molecule that requires binding through residue 37 to induce NFκB activation and CL-1 expression, thus pointing to a novel mechanism for induction of ROS.

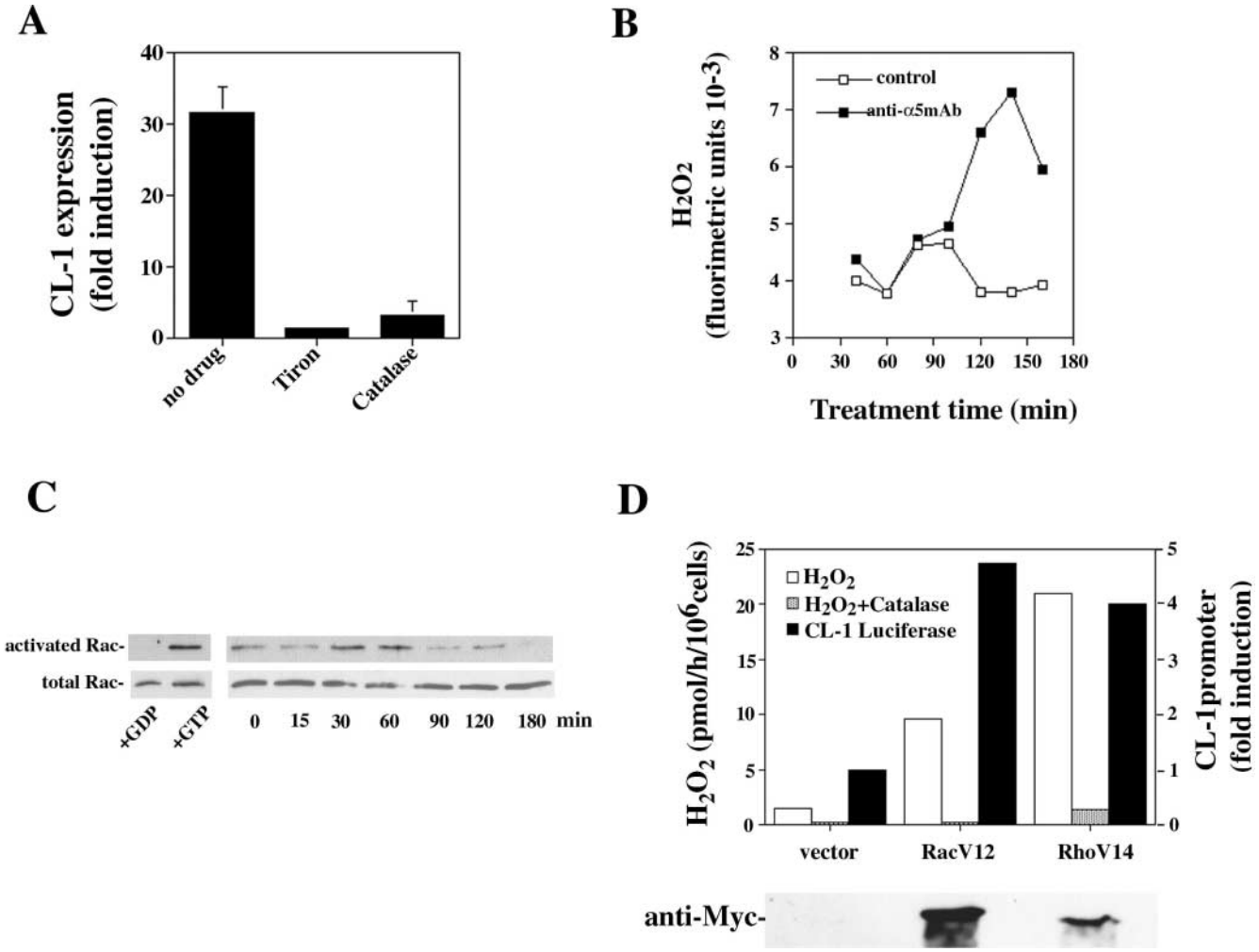

Figure 1. **Anti-α5 mAb induces H_2O_2 production and Rac activation.** (A) Anti-α5 mAb induces CL-1 expression by an oxidant-dependent mechanism. Cells were incubated in the absence or presence of 1 mM Triton or 200 U/ml catalase with 10 μg/ml anti-α5β1 mAb. After 24 h, CL-1 production was measured by slot blot analysis of the supernatants. This is one of three experiments. (B) Anti-α5 mAb induces a transient increase in H_2O_2 production. Cells were incubated for different intervals without or with anti-α5β1 mAb, and H_2O_2 production was measured. One of twelve experiments is represented. (C) Anti-α5 mAb induces transient activation of endogenous Rac. Cells were incubated for different intervals without or with 10 μg/ml anti-α5 mAb. An aliquot (1/10) of the lysate was separated to measure total Rac, and the rest was incubated with the Rac-binding domain of PAK-agarose to isolate activated Rac. The amount of precipitated Rac was determined by Western blotting. One of two experiments is represented. (D) Constitutively activated Rac and RhoA induce H_2O_2 production and CL-1 induction. RSFs were transiently transfected with RacV12, RhoV14, or empty vector (vector) and the CL-1 promoter–luciferase construct. After 48 h of transfection, H_2O_2 production in the absence and presence of 20 U/ml of catalase was measured, and luciferase activity was determined in cell lysates.

While mutants in residue 37 disrupt several Rac-dependent cytoskeletal events, they do not abolish JNK or PAK activation (Nobes and Hall, 1995; Joneson et al., 1996; Westwick et al., 1997). We found that although the RacV12 L37 mutant abrogated Rac-induced reorganization of the actin cytoskeleton (Fig. 2 C), it still activated JNK (Fig. 2 D) as it has been described before (Joneson et al., 1996; Lamarche et al., 1996). RSFs transfected with the L37 mutant maintained a fibroblast-like morphology and extensive stress fibers without visible lamellipodia formation and actin reorganization. In contrast, RacV12-transfected cells changed shape, adopting a dish-like round morphology with abundant lamellipodia at the cellular edges and actin filaments organized into a subcortical array rather than into stress fibers. The H26 and N130 mutants showed a RacV12-like phenotype. Together with the observation that activated RhoA can also induce ROS and CL-1 production, these results further support our conclusion that Rac-mediated ROS production is by a mechanism different from the activation of a membrane oxidase. In keeping with these observations, the flavoprotein inhibitor diphenylene iodonium did not inhibit integrin-induced CL-1 expression (unpublished data).

Mitochondria are the source of integrin-mediated ROS production

An important source of ROS is the nonenzymatic generation of superoxide as a by-product of mitochondrial metabolism. In our assay, the H_2O_2 signal was inhibited when the cells were preincubated with a superoxide scavenger, Tiron, and abolished by the simultaneous addition of catalase to the reaction mixture (Fig. 3 A), corroborating that the detected signal is effectively H_2O_2 and suggesting that the H_2O_2 is

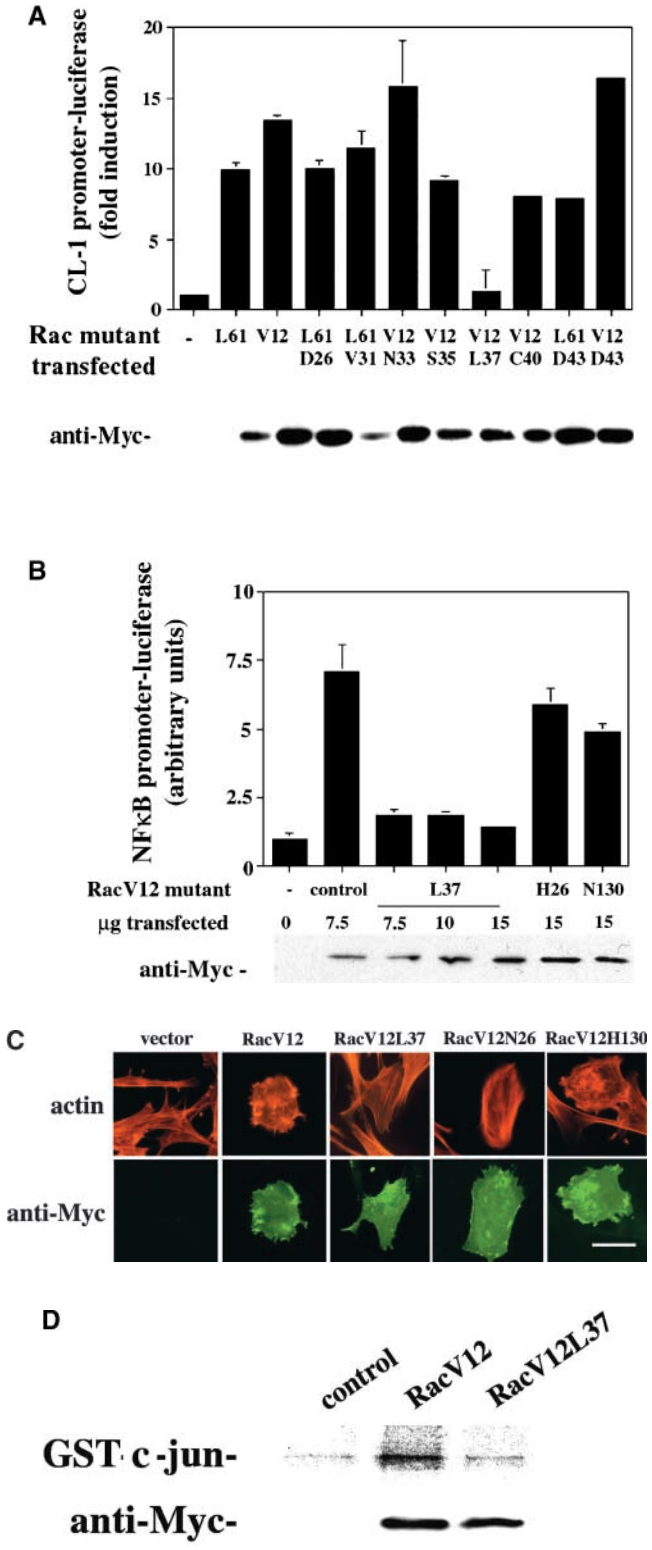

Figure 2. **Activated Rac induces ROS production through a novel mechanism**. (A) Effect of point mutations in the effector domain of RacV12 on signal transduction. A series of effector domain point mutants on RacV12 or RacL61 backbones were cotransfected with a CL-1 promoter–luciferase construct into RSFs, and luciferase activity was measured 72 h later. The bottom panel shows the expression of the myc-tagged Rac constructs in 2×10^4 cells. This experiment is representative of four. (B) Effect of RacV12RacV12L37 and RacV12 mutants that are unable to interact with the neutrophil oxidase in vitro on NFκB activation. RSFs were transiently cotransfected with RacV12 or RacV12 containing the point mutations L37, H26, or N130 plus a NFκB promoter–luciferase construct, and luciferase activity was measured 72 h later. The bottom panel shows the expression of the myc-tagged Rac constructs in 2×10^4 cells. This experiment is representative of four. (C) Effect of RacV12 point mutants on the actin cytoskeleton organization. Fluorescence microscopy of cells transfected with Myc-tagged Rac mutants and immunostained for the Myc tag (green) and for actin (red). Bar, 50 μm. (D) Effect of RacV12 and the L37 mutant on JNK kinase activation. Cos 7 cells were transiently transfected with empty vector (control), RacV12, or RacV12L37. After 24 h in the absence of serum, endogenous JNK was immunoprecipitated, and kinase activity was measured using GST–c-jun as a substrate and revealed by autoradiography.

originated by superoxide. The H_2O_2 signal induced by anti-α5 mAb was abrogated by inhibition of the function of mitochondrial respiratory chain complex 1 by 1 μM rotenone, complex 3 by 25 μM antimycin A, or complex 4 by 500 μM KCN (Fig. 3 A). These results suggest that the mitochondrial respiratory chain is responsible for the rise in ROS induced by anti-α5 mAb.

Tetrazolium salts are reduced to formazan by superoxide in vitro (Flohe and Otting, 1984) and by dehydrogenases and reductases in tissues. Therefore, they have been used as an indicator of mitochondrial metabolism and for succinate dehydrogenase (Powers et al., 1993). As an alternative strategy to evaluate mitochondrial metabolic/redox function, we incubated RSFs with nitroblue tetrazolium (NBT), which generates an insoluble formazan upon reduction. Anti-α5 mAb induced an increase in NBT precipitate associated with an intracellular membranous compartment (Fig. 3 B). The observed staining was dependent on mitochondrial function, since it was inhibited by rotenone, and was dependent on reduction, since it was inhibited by 10 mM *N*-acetyl-L-cysteine. Furthermore, we analyzed whether RacV12 expression promotes NBT precipitation. To do this experiment, RacV12 was cotransfected with histone 2B–GFP to mark the transfected cells. When used in a 2:1 ratio, 75% of the cells expressing GFP coexpressed RacV12 evidenced by immunofluorescence (unpublished data). In these cells, RacV12 induced NBT precipitation associated with an intracellular membranous compartment of similar distribution to that induced by anti-α5 mAb (Fig. 3 C). Quantification of the NBT precipitate by solubilization showed a significant ($P < 0.05$) increase in NBT precipitation induced by RacV12 but not by RacV12L37 or RacN17 (Fig. 3 D). Considering that only a subset of RSFs express the Rac mutants in these transiently transfected cultures, these data indicate a strong influence of activated Rac in mitochondrial metabolic/redox function. Together, these results suggest that integrins modify mitochondrial function to produce ROS by a novel Rac-dependent mechanism.

Because the diversion of electrons to form superoxide can lead to a dissipation of membrane potential ($\delta\Psi$) (Zoratti and Szabo, 1995; Madesh and Hajnoczky, 2001), we examined whether integrin cross-linking induces changes in mitochondrial membrane potential. We analyzed the distribution of the dual emission potentiometric probe JC-1. When high negative potential drives the dye concentration above a threshold, the green fluorescent monomers (low membrane potential) form red fluorescent aggregates (high membrane

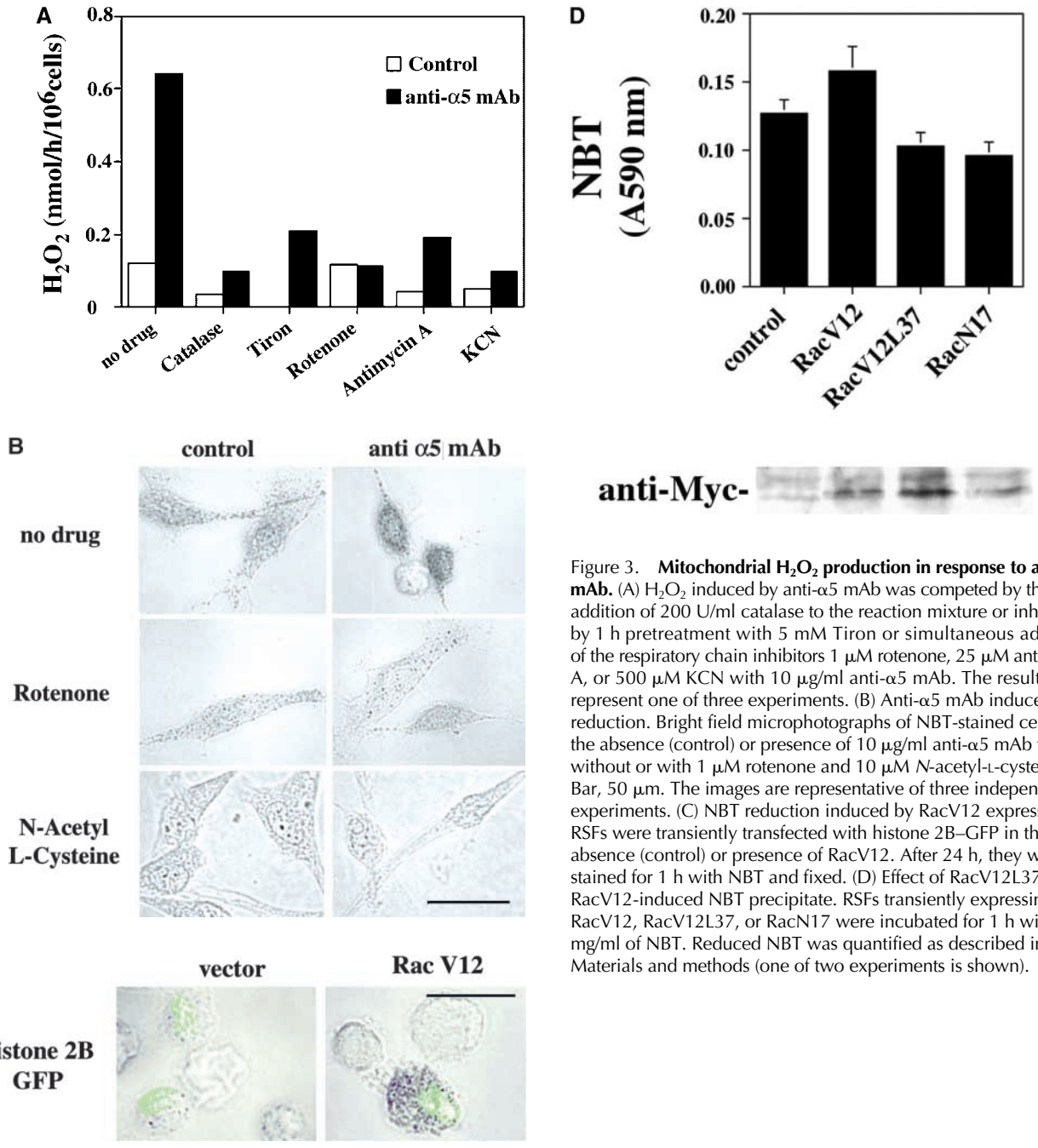

Figure 3. **Mitochondrial H_2O_2 production in response to anti-α5 mAb.** (A) H_2O_2 induced by anti-α5 mAb was competed by the addition of 200 U/ml catalase to the reaction mixture or inhibited by 1 h pretreatment with 5 mM Tiron or simultaneous addition of the respiratory chain inhibitors 1 μM rotenone, 25 μM antimycin A, or 500 μM KCN with 10 μg/ml anti-α5 mAb. The results represent one of three experiments. (B) Anti-α5 mAb induces NBT reduction. Bright field microphotographs of NBT-stained cells in the absence (control) or presence of 10 μg/ml anti-α5 mAb treated without or with 1 μM rotenone and 10 μM *N*-acetyl-L-cysteine. Bar, 50 μm. The images are representative of three independent experiments. (C) NBT reduction induced by RacV12 expression. RSFs were transiently transfected with histone 2B–GFP in the absence (control) or presence of RacV12. After 24 h, they were stained for 1 h with NBT and fixed. (D) Effect of RacV12L37 on RacV12-induced NBT precipitate. RSFs transiently expressing RacV12, RacV12L37, or RacN17 were incubated for 1 h with 0.3 mg/ml of NBT. Reduced NBT was quantified as described in Materials and methods (one of two experiments is shown).

potential). After 15 min of dye loading at 37°C, most of the mitochondria in control RSFs were bright orange (Fig. 4 A, a), indicative of highly energized mitochondria. When the membrane potential was dissipated with the protonophore FCCP, all of the mitochondria stained green (Fig. 4 A, f), corroborating that JC-1 accumulation is driven by membrane potential. After 2 h of anti-α5 mAb treatment, a population of cells had only green-stained mitochondria (Fig. 4 A, c). Frequently, the green staining mitochondria were present in cells that had rounded in response to the anti-α5 mAb treatment. The number of cells with green-stained mitochondria increased with time from 7 ± 1% (SEM) at 0 h to 21 ± 4% after 2 h and to 43% after 8 h of anti-α5 mAb addition. However, by 24 h the mitochondria in all cells were highly polarized again (Fig. 4 A, e), and no cells with only green mitochondria were detected, indicating that this is a reversible change. Cytochalasin D, which also induces ROS production (Kheradmand et al., 1998), induced mitochondrial depolarization after 2 h of treatment (Fig. 4 A, b). These results further support the biochemical evidence for cell shape–dependent control of mitochondrial function.

But are the observed changes in mitochondrial potential linked to the signal transduction cascade triggered by anti-α5 mAb? We analyzed whether the cells with depolarized mitochondria after anti-α5 mAb treatment are the same ones that are induced to express CL-1. We treated RSFs with anti-α5 mAb for 4 h and stained them with JC-1 for 15 min at 37°C. We then separated two populations of cells according to their

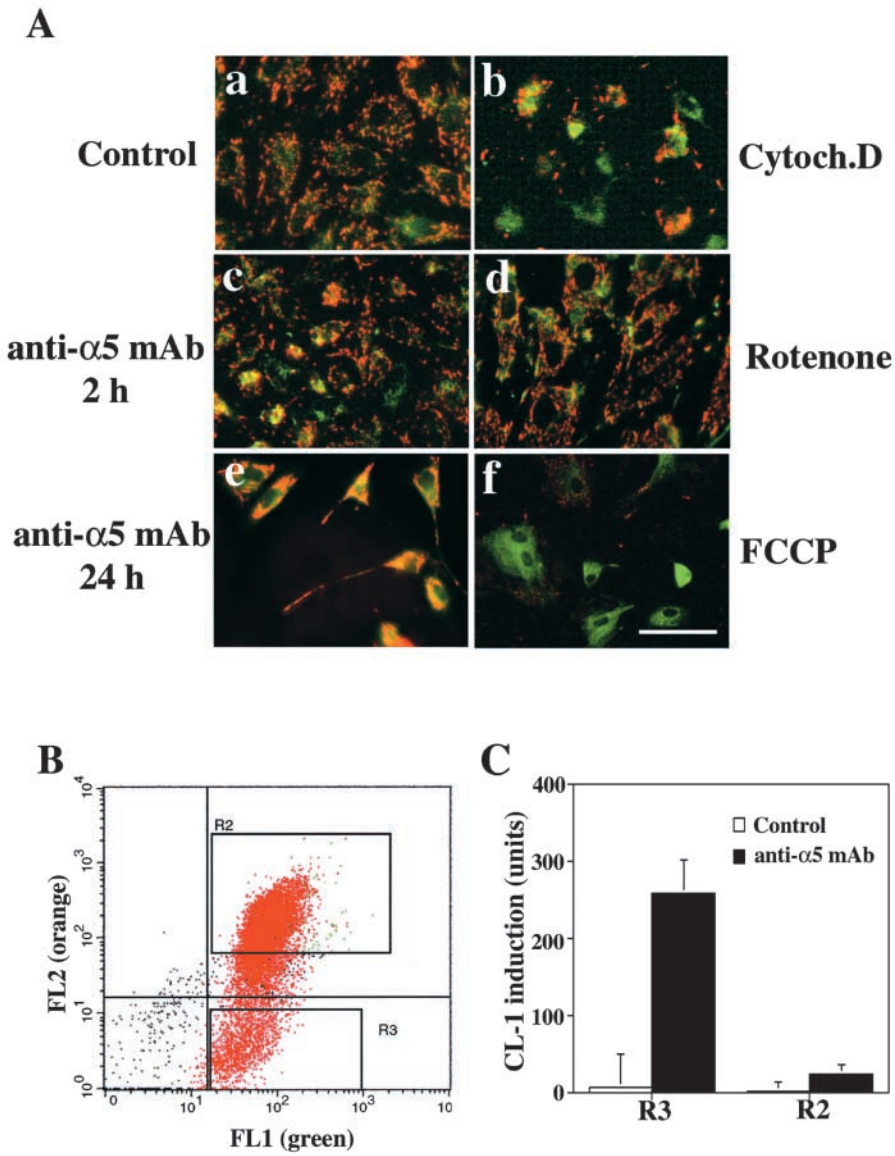

Figure 4. **Mitochondrial depolarization and CL-1 induction.** (A) Fluorescence microscopy of RSFs stained with JC-1. Fibroblasts treated without (a), or with 10 μM FCCP (f) for 2 h (c), or 24 h (e) with 10 μg/ml anti-α5 mAb, 2 μg/ml cytochalasin D for 2 h (b) or 1 μM rotenone for 2 h (d) were stained with JC-1. Bar, 25 μm. High potential mitochondria (>−140 mV) stain red; low potential (−100 mV) mitochondria stain green. Bar, 50 μm. (B) Dot plot graph of FACS® analysis of RSFs treated for 4 h with anti-α5 mAb and stained with JC-1 for 15 min at 37°C. The cells with only green fluorescence (R3) and the cells with highest red emission (R2) were sorted from control and anti-α5 mAb–treated populations, and equal numbers were plated for 24 h on fibronectin. (C) CL-1 protein produced by each population of cells was measured by slot blot.

mitochondrial staining using fluorescence-activated cell sorting, gating to isolate cells with depolarized (green) mitochondria from polarized (orange) mitochondria (Fig. 4 B). Equal numbers of cells with depolarized mitochondria (green) or with polarized mitochondria (orange) were plated on glass coverslips and analyzed for CL-1 expression 24 h later. We found that background and anti-α5 mAb–induced CL-1 expression segregated with the cells that had depolarized mitochondria 24 h earlier (Fig. 4 C). Although very few cells with depolarized mitochondria were obtained from control cultures, those cells did make low levels of CL-1 seen as basal levels, whereas the cells with polarized mitochondria did not. These results demonstrate that the cells showing mitochondrial membrane depolarization are committed to CL-1 expression.

Bcl-2 blocks integrin-mediated signaling for CL-1 expression

Cell rounding and detachment can induce apoptosis in some cell types (Ruoslahti and Reed, 1994). During the induction of apoptosis, mitochondria are engaged to produce ROS and undergo membrane depolarization, membrane permeability transition (MPT), release of specific proteins from the intermembrane space (cytochrome C, procaspases 2 and 9, Apaf-1, and AIF), and caspase activation through a mechanism that is not clear (Kroemer and Reed, 2000). Members of the Bcl-2 family can inhibit ROS production (Hockenbery et al., 1993; Kane et al., 1993), membrane potential loss (Gottlieb et al., 2000), MPT (Marzo et al., 1998), cytochrome C release (Yang et al., 1997), and caspase activation (Strasser et al., 2000). We hypothesized that in response to triggering integrin-mediated signaling in RSFs the mitochondrial signal transduction is engaged by a mechanism common to apoptosis, yet is resolved into induction of gene expression instead of cell death.

Neither control cells nor cells treated for 4 h with anti-α5 mAb showed cytochrome C release from mitochondria to the cytosol by Western blot analysis (Fig. 5 A) or by immunofluorescence (unpublished data). The addition of selective inhibitors of caspases 1 or 3 or the general caspase inhibitor Z-VAD fluoromethyl ketone did not inhibit anti-α5 mAb–induced CL-1 production (Fig. 5 B), although they effectively inhibited staurosporine-induced apoptosis (unpublished data). Anti-α5 mAb induced equivalent amounts of

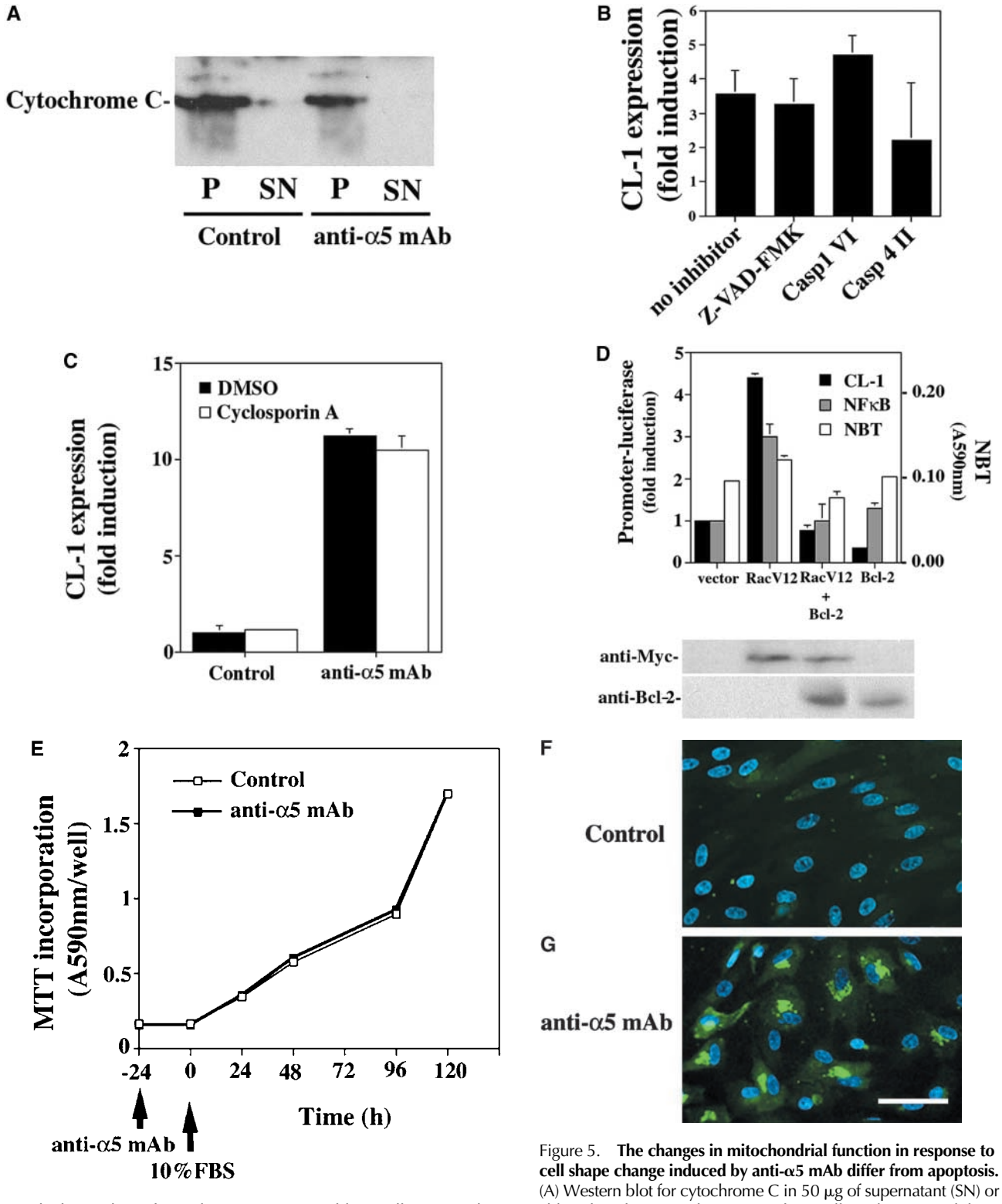

Figure 5. **The changes in mitochondrial function in response to cell shape change induced by anti-α5 mAb differ from apoptosis.** (A) Western blot for cytochrome C in 50 μg of supernatant (SN) or 100 μg high speed membrane fraction (P) prepared from cells untreated or treated for 4 h with 10 μg/ml anti-α5 mAb. (B) Effect of caspase inhibitors on anti-α5 mAb–induced CL-1 expression. RSFs were incubated for 30 min with 200 μM Z-VAD–FMK, caspase 1 inhibitor VI, caspase 4 inhibitor II, or DMSO followed by addition of anti-α5 mAb. After 24 h, CL-1 in the supernatant was measured by slot blot. (C) Effect of cyclosporin A on CL-1 expression induced by anti-α5 mAb. RSFs were incubated for 30 min with 20 μM cyclosporin A or DMSO followed by addition of anti-α5 mAb. After 24 h, CL-1 in the supernatant was measured by slot blot. (D) Human Bcl-2 inhibits RacV12-induced NFκB activation, CL-1 expression, and NBT precipitation. RSFs were cotransfected with empty vector or RacV12 or hBcl-2, and constructs for β-galactosidase, NFκB, or CL-1 promoters coupled to luciferase. After 48 h of transfection, luciferase and β-galactosidase activity were measured in the cell lysates. The results are corrected by transfection efficiency using β-galactosidase activity as reference. This experiment represents one of three. (E) Effect of anti-α5 mAb on cell viability: growth curve upon serum restitution after anti-α5 mAb treatment. Cells were treated for 24 h without or with 10 μg/ml of anti-α5 mAb in serum-free medium (0.2% LH). RSFs were replated and grown in 10% FBS. After different intervals, MTT incorporation was measured. Each point represents the average of triplicates with the error bars too small to appear represented. (F and G) Fluorescence microscopy of RSFs expressing CL-1. Immunostaining for CL-1 (green) and costaining with DAPI (blue) in cells incubated (F) without or (G) with 10 μg/ml of anti-α5 mAb for 24 h. Bar, 100 μm.

CL-1 in control cells or cells treated with an inhibitor of MPT, cyclosporin A (Fig. 5 C). In contrast, we found that Bcl-2, which blocks several mitochondrial-dependent processes during apoptosis, inhibited integrin ligation-induced signal transduction. The transient overexpression of human Bcl-2 in RSFs inhibited RacV12-induced NBT precipitation as a measure of mitochondrial metabolic/redox function and transcriptional activation of both NFκB and CL-1 promoters (Fig. 5 D). Importantly, the anti-α5 mAb treatment did not induce apoptosis at 24 h cells cultured without serum as analyzed by the TUNEL method (unpublished data) or by growth rates upon serum restitution as measured by dimethylthiazolyldiphenyltetrazolium bromide (MTT) metabolism (Fig. 5 E). After 24 h of anti-α5 mAb treatment, all of the cells expressing CL-1 exhibited a normal nuclear morphology by DAPI staining, confirming that CL-1 induction is not associated with cell death (Fig. 5, F and G). Together, these results further support a role for mitochondria in integrin-dependent signal transduction by a mechanism that can be regulated by Bcl-2 but that is different from apoptosis.

Discussion

We have shown here that integrins activate Rho GTPase function to produce ROS for signal transduction production by a novel mechanism different from the activation of a plasma membrane NADPH oxidase. Downstream of Rac, the pathway engages mitochondria as a signaling center for processes distinct from apoptosis.

Integrin control of mitochondrial function

Four independent lines of evidence advocate a role for mitochondria in integrin-induced signal transduction. The first line of evidence for mitochondrial involvement in signal transduction is anti-α5 mAb–induced mitochondrial depolarization in cells committed to CL-1 gene expression.

Second, we found that integrin cross-linking induces a ROS increase that requires the function of complexes 1, 3, or 4 of the respiratory chain. Glycolysis maintains the levels of ATP upon inhibition of the respiratory chain in primary fibroblasts (McKay et al., 1983). Thus inhibition of respiration does not hinder the mitochondrial pathway by causing ATP depletion. In confirmation, blocking mitochondrial respiration with rotenone alone was not sufficient to cause mitochondrial depolarization due to reverse activity of the ATP synthase. In isolated mitochondria, complexes 1 and 3 participate directly in ROS production. NADPH or succinate induces superoxide production under conditions of slow respiration (state 4, not conductive to ATP synthesis) where the reduced state of the ubisemiquinone favors the direct transfer of electrons to oxygen (Turrens et al., 1985). Antimycin A enhances but rotenone and cyanide inhibit this mechanism. Although integrin-induced ROS production was sensitive to rotenone and cyanide, we could not detect enhanced ROS production induced by antimycin A. This deviation can be explained by differences in the mitochondrial metabolic state or in antimycin A sensitivity of intact cells. Alternatively, the site for superoxide production could be at cytochrome B or downstream of the antimycin A block. Such a mechanism has been invoked for ROS production induced by release of cytochrome C to the cytosol during apoptosis (Cai and Jones, 1998; Sanchez-Alcazar et al., 2000). However, this mechanism seems unlikely because we did not detect cytochrome C release, indicating the existence of a different mechanism.

The third line of evidence for mitochondrial participation in integrin-mediated signal transduction comes from the increase in anti-α5 mAb–induced NBT reduction into insoluble formazan. Even though tetrazolium salts can be reduced by several dehydrogenases, the results are consistent with NBT reduction in mitochondria. We found that NBT reduction occurs at the same time of the detected rise in H_2O_2 production (unpublished data) and distributes into an intracellular and vesicular compartment. RacV12, which induced H_2O_2 production and signal transduction, was sufficient to induce a similar staining pattern. Additionally, formazan deposition was abolished by interfering with mitochondrial function using rotenone and inhibited by the effector domain mutant L37 or by Bcl-2 when induced by RacV12.

A fourth line of evidence constitutes Bcl-2 inhibition of RacV12 signaling. Although Bcl-2 localizes to mitochondria, nucleus, and ER, its inhibition of NBT reduction manifests a role in the control of mitochondrial homeostasis. Accordingly with this view, accumulating evidence indicates that rather than antagonizing specific steps of apoptosis Bcl-2 regulates mitochondrial metabolism, including ADP/ATP exchange (Vander Heiden et al., 1999), permeability to metabolic anions (Vander Heiden et al., 2000), and preventing membrane potential dissipation by increasing proton efflux (Shimizu et al., 1998). These mechanisms predict the participation of Bcl-2 in nonapoptotic processes. Interestingly, overexpression of Bcl-xL in pancreatic islet β cells inhibits not only apoptosis but also mitochondrial response to glucose (Zhou et al., 2000). Thus, the simplest interpretation for our results is that Bcl2 interferes with signal transduction by counteracting Rac-induced changes in mitochondrial metabolism.

Rac mediates ROS production through a novel mechanism

We show that integrins engage mitochondria through the activation of Rac, which constitutes a novel mechanism for this GTPase to mediate ROS production. We have shown previously that integrin ligation induces ROS production by a Rac-dependent mechanism (Kheradmand et al., 1998). Now we show that this GTPase is activated downstream of integrin cross-linking before ROS levels increase at 2 h. These nonoverlapping kinetics suggest a novel indirect mechanism for Rac-dependent ROS induction, involving one or more intermediate steps after the GTPase activation. This mechanism is further supported by our observation that RhoA, although unable to activate the neutrophil oxidase (Abo et al., 1991), also induces H_2O_2 and CL-1 production in RSFs. This is not as a result of cross-talk between the GTPases because integrin-mediated signaling is selectively inhibited by interfering with the function of one of the GTPases, i.e., only RacN17 inhibits anti-α5 mAb signaling (Kheradmand et al., 1998) and only RhoA N19 interferes with integrin-mediated phagocytosis signaling (Werner et al., 2001). Our findings with the effector domain mutants of Rac further support an indirect mechanism distinct from the activation of a membrane oxidase.

Our results indicate that Rho GTPases modulate mitochondrial function through an indirect mechanism, which could involve the control of the anti/proapoptotic function of the Bcl-2 family members and/or the organization of the cytoskeleton. Integrins can engage multiple mechanisms that could sustain cell survival by controlling the function of different members of the Bcl-2 family. Phosphatidylinositol 3-kinase, which can be activated by Rac (Bokoch et al., 1996), activates PKB/Akt kinase and modulates the apoptotic function of Bad (del Peso et al., 1997). However, in our system inhibitors of phosphatidylinositol 3-kinase did not affect anti-α5 mAb–induced signaling (unpublished data), suggesting that signaling proceeds by a different mechanism. Integrins can also restrict Bax localization during epithelial cell adhesion to extracellular matrix (Gilmore et al., 2000). An additional mechanism implied in the literature, but not yet demonstrated, is the control of the function or localization of members of the Bcl-2 family by integrins through interaction with members of the 14-3-3 scaffolding protein family. These proteins have multiple interaction partners including β1 integrins during cell spreading (Han et al., 2001) and p190RhoGEF (Zhai et al., 2001). On the other end of the cascade, the interaction of 14-3-3 with Bad prevents its proapoptotic function (Datta et al., 2000).

Alternatively, this indirect mechanism could involve the actin cytoskeleton. Rac induction of ROS production through a signal conveyed by reorganization of the actin cytoskeleton is consistent with the ability of cytochalasin D (Kheradmand et al., 1998) and activated RhoA to induce H_2O_2 and CL-1 production. A tantalizing candidate to couple mitochondrial function to actin cytoskeleton reorganization is gelsolin, a member of a multigene family of proteins with actin filament severing and capping activity. In preliminary studies, we have found that microinjection of gelsolin protein into RSFs induces shape change, motility, and expression of CL-1 (unpublished data). Gelsolin is a downstream target of Rac in fibroblasts (Azuma et al., 1998) and neutrophils (Arcaro, 1998). Gelsolin inhibits caspase activation (Azuma et al., 2000) and modifies mitochondrial membrane potential by modulating VDAC activity (Kusano et al., 2000), thus inhibiting apoptosis (Koya et al., 2000). Gelsolin may also be involved in signal transduction, since null fibroblasts have a blunted proinflammatory response (Witke et al., 1995). Interestingly, in RSFs, integrin-mediated activation of Rho and Rac and ROS production induces the expression of proinflammatory cytokines through activation of NFκB (Kheradmand et al., 1998; Werner et al., 2001).

Together, we favor a model for the participation of mitochondria in integrin signaling in a nonapoptotic cascade that leads to gene expression and cell differentiation.

Inhibition of integrin (this paper) and RacV12 (Kheradmand et al., 1998) signaling by antioxidants indicates that mitochondria are engaged to generate superoxide as an intermediary in the signal transduction pathway. We also found that in cells committed to signaling mitochondria undergo membrane depolarization. Our results are insufficient to demonstrate a direct relationship between both mitochondrial changes. However, the time course of both events (at the time we observe a sharp decrease in H_2O_2 production, we still detect an increase in the number of cells with depolarized mitochondria) indicates that superoxide is produced first, and then membrane potential is lowered. This order of events would be consistent with the known mitochondrial superoxide production dependency from membrane potential (Korshunov et al., 1997) and the regulation of VDAC function by superoxide (Zoratti and Szabo, 1995; Madesh and Hajnoczky, 2001). Further experiments are needed to demonstrate the soundness of this model.

Few other examples exist showing that mitochondria participate in signal transduction by capturing Ca^{+2} or producing ROS (for review see Duchen, 1999). In most cases, ROS production and membrane potential loss have been associated with apoptosis. However, induction of apoptosis and gene expression appear to share a common pathway of signaling through mitochondria where the outcome is dictated by survival signals. It is instructive to compare the integrin-triggered pathway with TNFα-induced signal transduction. TNFα-induced apoptosis has been studied mainly in cells treated with cycloheximide or actinomycin D where the absence of survival pathways provided by the activation of gene expression shifts the outcome of signaling to cell death. However, in most normal cell types TNFα induces gene expression through the activation of NFκB, AP-1, JNK, and MAPKK by a mechanism dependent on mitochondrial respiratory chain function (Schulze-Osthoff et al., 1993; Goossens et al., 1995), a pathway that is abrogated by stable manganese superoxide dismutase overexpression (Manna et al., 1998). Rac is also part of these dual pathways. Its activity is necessary both for TNFα-mediated apoptosis (Embade et al., 2000) and gene expression (Esteve et al., 1998). Apoptosis induced by altered adhesion and FAK function can be compensated by Rac activation (Almeida et al., 2000). The participation of Rac and mitochondria in these pathways with dual outcomes suggests that an additional signal is required. This interpretation is consistent with observations that Rho and Rac can mediate apoptosis in the absence of survival signals from serum (Esteve et al., 1998; Embade et al., 2000) or mediate cell proliferation and transformation in the presence of these signals.

By largely unexplored mechanisms, mitochondrial function must be coupled to other cellular functions to accommodate changes in metabolism requirements. Mitochondria could be recruited to respond to new metabolic requirements by controlling ATP levels or lipid metabolism or, as it is in this case, to promote oxidative signaling. More interestingly, mitochondria may coordinate parallel signal transduction pathways triggered by the altered cytoarchitecture that takes place during changes in tissue organization, cell locomotion, inflammatory responses, wound healing, or tumor progression. It is interesting to note that many tumor cells have altered mitochondrial function with increased glycolytic metabolism, a process known as the Warburg effect (Racker, 1983). Altered adhesion and activation of Rac and Rho GTPase isoforms are also features of many tumor cells. Whether these processes are functionally coupled remains to be determined.

Materials and methods

Reagents

Rac activation assay kit was obtained from Upstate Biological, luciferase assay kit was from Promega, β-galactosidase assay kit was from Tropix, hu-

man fibronectin was from Roche, and anti–cytochrome C was from BD PharMingen. FCCP, rotenone, antimycin A, KCN, MTT, cyclosporin A, cytochalasin D, peroxidase, homovanillic acid, Tiron, NBT, and H_2O_2 were obtained from Sigma-Aldrich. JC-1, rhodamine-conjugated phalloidin, and Alexa-conjugated secondary antibodies were obtained from Molecular Probes. Catalase, Z-VAD-FMK, Casp1 VI, Casp 4 II, and *N*-acetylcysteine were obtained from Calbiochem.

Cells

RSFs were isolated as described previously (Aggeler et al., 1984) and cultured between passages 3 and 10 in DME H-21 supplemented with 10% FBS (Hyclone) and 2 mM glutamine in 5% CO_2 at 37°C. For the experiments, RSFs from confluent cultures were plated in DME supplemented with 0.2% lactalbumin hydrolysate (LH) on dishes coated previously for 2 h with 20 μg/ml of human fibronectin in PBS and then blocked for 30 min with 0.2% LH-DME. After 1 h to allow cell spreading, 10 μg/ml of protein G–affinity-purified anti-α5 mAb (BIIG2, a gift from Dr. C. Damsky, University of California, San Francisco, CA) was added. As controls, purified rat immunoglobulins or unrelated antibodies of the same species and isotype were used.

H_2O_2 assay

Confluent RSFs were plated on fibronectin-coated plates for at least 4 h before the experiments. Anti-α5 mAb was added at 20-min intervals, and at the end the cells were washed with PBS and incubated with Hank's balanced salt solution without phenol red, 1 mM Hepes, 100 μM homovanillic acid, and 5 U/ml HRP type VI for 1 h at 37°C (Baggiolini et al., 1986). The samples were alkalinized with 0.1 M glycine-NaOH, pH 10, and the formation of the fluorescent product was measured in a Fluorolog 3 Instruments SA fluorimeter at excitation of 321 nm and emission at 421 nm. No reading was detected when peroxidase or substrate was omitted. Standards were prepared from a 30% wt/vol H_2O_2 stock solution. The limit of detection was 0.05 μM, whereas the basal activity detected was 0.1 μM. The amount of H_2O_2 produced was calculated by adding the three readings where anti-α5 mAb–induced H_2O_2 production peaked. The respiratory chain inhibitors were added at the first time of anti-α5 mAb addition (2.2 h). After the PBS wash, the residual amount of inhibitors did not interfere with the reading of a standard amount of H_2O_2 added (unpublished data). The readings were corrected for cell number.

Rac activation assay

To measure Rac activation, confluent cultures were cultured overnight in DME-LH. RSFs (5×10^6) were plated on fibronectin-coated plates for 4 h and then incubated with 10 μg/ml of anti-α5 mAb for different periods. Cells were lysed in 500 μl of lysis buffer and 450 μl incubated with PAK1-RBD agarose following the manufacturer recommendations (Upstate Biotechnology). The total Rac present in the lysate was measured in 50 μl before incubation with PAK1-RBD and activated Rac bound to PAK-RBD were detected by Western blot.

JNK kinase assay

Transfected Cos 7 cells were lysed in 20 mM Tris, pH 7.6, 250 mM NaCl, 3 mM EDTA, 20 mM β glycerophosphate, 0.5% (vol/vol) NP-40, 1 mM DTT, 1 mM sodium orthovanadate, and protease inhibitors. JNK was immunoprecipitated for 2 h with anti-JNK antibody (Cell Signaling) and washed two times with kinase buffer. The immune complex-associated kinase activity was measured in kinase buffer (25 mM Hepes, pH 7.5, 20 mM β glycerophosphate, 2 mM DTT, 20 mM $MgCl_2$, 0.1 mM sodium orthovanadate) incubated with 1 μg GST-c-jun and 5 μCi [γ-^{35}S]ATP for 30 min at 30°C. After gel electrophoresis, c-jun phosphorylation was revealed by autoradiography (Sudo and Karin, 2000).

NBT staining

RSFs were incubated for 1 h at 37°C with a filtered solution of 0.3 mg/ml of NBT in Hank's balanced salt solution without phenol red during the second hour of anti-α5 mAb treatment. These conditions were established to optimize signal over the background differences in staining. The cells were washed once with PBS and fixed with 0.4% paraformaldehyde for light microscopy. To quantify NBT precipitation, cells were washed twice with 70% methanol and fixed for 5 min in 100% methanol. After the wells are allowed to air dry, the formazan is solubilized with 120 μl 2M KOH and 140 μl DMSO. The OD was read in an ELISA plate reader at 590 nm (Rook et al., 1985).

JC-1 staining

RSFs were plated on glass coverslips coated with fibronectin and were stained with 10 μg/ml of JC-1 in 0.2% LH DME for 15 min at 37°C (Smiley et al., 1991). JC-1 is a hydrophobic carbocyanine compound with delocalized positive charge that allows its cellular distribution driven by negative potential; when the concentration reaches a threshold, it forms aggregates with a shift in the absorbed and emitted fluorescence. Therefore, when the membrane potential is < -100 mV the mitochondria appear green, but under conditions of high membrane potential (< -140 mV) high amounts of JC-1 aggregate and form a red fluorescent complex (Smiley et al., 1991). Cells were photographed within 5 min under epifluorescence using a FITC/TR dual band pass filter in a Leica DMR microscope.

For the cell isolation experiments, RSFs were treated for 4 h without or with 10 μg/ml of anti-α5 mAb, stained with JC-1 for 15 min at 37°C, and then released with trypsin-EDTA. Soybean trypsin inhibitor was added, and the cells were sorted in a Becton Dickinson FACSVantage SE cell sorter gated to separate cells by green and orange fluorescence. 5×10^5 cells collected from each condition were plated on fibronectin-coated glass coverslips and then incubated for an additional 24 h. Secreted CL-1 in the supernatant was measured by slot blot. The number of cells recovered after 24 h was confirmed by counting nuclei after staining with DAPI.

Cytochrome C release

RSFs were incubated for 4 h without or with 10 μg/ml of ant-α5 mAb and homogenized as described (Carthy et al., 1999). Cytochrome C was detected by Western blot analysis of protein in the high speed pellet (100 μg of protein) for mitochondria and supernatant (50 μg) for cytosol.

MTT assay

To quantify viable cells, 20 μl of 5 mg/ml MTT in PBS was added to 100 μl of culture medium and incubated with RSFs at 37°C for 1 h. Metabolized MTT was solubilized with 300 μl of DMSO, and color development was measured at 570 nm. Each point shown is the average of triplicates with a standard deviation too small to be represented in the graph.

Western and slot blot

CL-1 expression was measured by slot blot analysis of serial dilutions of the treated cell culture supernatants as described previously or by Western blot analysis of the cell culture supernatants using a mixture of six monoclonal anti–rabbit CL-1 mAb (oligoclonal) and an HRP-conjugated anti–mouse secondary antibody (Tremble et al., 1994). HRP binding was evidenced by enhanced luminescence reaction, and the bands were quantified by densitometry using Image Quant software for analysis. The reference value to calculate fold of induction was the basal expression of CL-1 of cells plated on fibronectin without anti-α5 mAb.

Immunofluorescence

The cells were plated on fibronectin-coated glass coverslips. The monolayer was washed with PBS and fixed with 4% paraformaldehyde in PBS for 20 min, permeabilized with 0.1% Triton X-100 for 3 min, and blocked for 1 h with 15% FBS in PBS. Primary antibodies were diluted in 15% FBS and incubated for 1 h at 37°C. After three washes with PBS 0.1% Triton X-100, the samples were incubated with Alexa-labeled secondary antibodies (Molecular Probes) for 45 min and embedded in Vectashield with DAPI (Vector Laboratories). Samples were analyzed and photographed using a Leica DMR microscope.

Plasmids and transfections

Dr. Marc Symons (Picower Institute for Medical Research, Manhasset, NY) provided the expression plasmids with RhoA V14 (Qiu et al., 1995), and Dr. Gaston Hayes (Onyx Pharmaceuticals, Richmond, CA) provided the panel of Rac mutants (Westwick et al., 1997). The NFκB reporter plasmid corresponds to the ELAM promoter from –730 to +52 coupled to luciferase and was provided by Dr. Ulrike Schindler (Tularik Inc., South San Francisco, CA) (Schindler and Baichwal, 1994). To measure CL-1 induction, a minimal CL-1 promoter (−517 to 63) coupled to luciferase was used (Kheradmand et al., 1998). In control cells, empty vector or pEGFP1C (CLONTECH Laboratories, Inc.) was transfected in equal amounts. Dr. Stanley Korsmeyer (Dana Farber Cancer Institute, Harvard Medical School, Boston, MA) provided the expression vector with RSV-human Bcl-2 (Seto et al., 1988). The histone 2B–GFP construct is from Dr. Jennifer Lippincott-Schwartz (National Institutes of Health, Bethesda, MD).

The point mutants of RacV12 in the residues 26 and 130 were prepared using the QuickChange site Mutagenesis Kit (Stratagene). RacV12 in pcDNA3 was used as a template with the oligo 5′-CTGATCAGTTACACAACCCATGCATTTCCTGGAG-3′ to generate the H26 mutant and the oligo 5′-CGAGAAACTGAACGAGAAGAAGCTGACTCC-3′ to generate the N130 change. The mutations were verified by sequencing.

Cells were transfected using adenovirus as described previously (Forsayeth and Garcia, 1994) (Kheradmand et al., 1998). Briefly, the cells were

subcultured the day before. 3×10^6 cells were transfected in a 3.5-cm dish with 2.5 ml of the following mixture: adenovirus stock diluted 1:20 in serum and antibiotic-free DME, 2 μg/ml of plasmid, and 80 μg/ml DEAE-dextran. The cells and the mixture were incubated for 2 h at 37°C and then washed for 1 min with 10% DMSO in PBS and incubated overnight with DME 10% FBS. The medium was then changed to DME-0.1% LH and 24 h later. Equal numbers of cells were plated on fibronectin-coated dishes. The cells were analyzed after 24 h by measuring luciferase activity in whole cell lysates using a commercial kit (Promega). The readings were corrected by protein concentration (Bradford) or β-galactosidase activity (Tropix).

Data analysis

The experimental data are represented as means ± SEM. Statistical comparisons were performed using the two-tailed Student's *t* test. Values of $P < 0.05$ were considered to be statistically significant.

We thank Drs. Marc Symons and Gaston Hayes for providing plasmids and Bill Hyun at the University of California, San Francisco, Comprehensive Cancer Center for expert assistance with the cell-sorting experiments.

This work was supported by funds from the National Institutes of Health (AR20684 and CA72006) and the Ruth and Milton Steinbach Fund and a PEW International Fellowship to E. Werner.

Submitted: 8 November 2001
Revised: 12 April 2002
Accepted: 30 May 2002

References

Abo, A., E. Pick, A. Hall, N. Totty, C.G. Teahan, and A.W. Segal. 1991. Activation of the NADPH oxidase involves the small GTP-binding protein p21rac1. *Nature.* 353:668–670.

Aggeler, J., S.M. Frisch, and Z. Werb. 1984. Collagenase is a major gene product of induced rabbit synovial fibroblasts. *J. Cell Biol.* 98:1656–1661.

Almeida, E.A., D. Ilic, Q. Han, C.R. Hauck, F. Jin, H. Kawakatsu, D.D. Schlaepfer, and C.H. Damsky. 2000. Matrix survival signaling: from fibronectin via focal adhesion kinase to c-Jun NH(2)-terminal kinase. *J. Cell Biol.* 149:741–754.

Arcaro, A. 1998. The small GTP-binding protein Rac promotes the dissociation of gelsolin from actin filaments in neutrophils. *J. Biol. Chem.* 273:805–813.

Azuma, T., W. Witke, T.P. Stossel, J.H. Hartwig, and D.J. Kwiatkowski. 1998. Gelsolin is a downstream effector of rac for fibroblast motility. *EMBO J.* 17: 1362–1370.

Azuma, T., K. Koths, L. Flanagan, and D. Kwiatkowski. 2000. Gelsolin in complex with phosphatidylinositol 4,5-bisphosphate inhibits caspase-3 and -9 to retard apoptotic progression. *J. Biol. Chem.* 275:3761–3766.

Bae, Y.S., S.W. Kang, M.S. Seo, I.C. Baines, E. Tekle, P.B. Chock, and S.G. Rhee. 1997. Epidermal growth factor (EGF)-induced generation of hydrogen peroxide. Role in EGF receptor-mediated tyrosine phosphorylation. *J. Biol. Chem.* 272:217–221.

Baggiolini, M., W. Ruch, and P.H. Cooper. 1986. Measurement of hydrogen peroxide production by phagocytes using homovanillic acid and horseradish peroxidase. *Methods Enzymol.* 132:395–400.

Barrett, W.C., J.P. DeGnore, Y.F. Keng, Z.Y. Zhang, M.B. Yim, and P.B. Chock. 1999. Roles of superoxide radical anion in signal transduction mediated by reversible regulation of protein-tyrosine phosphatase 1B. *J. Biol. Chem.* 274: 34543–34546.

Benard, V., B.P. Bohl, and G.M. Bokoch. 1999. Characterization of rac and cdc42 activation in chemoattractant-stimulated human neutrophils using a novel assay for active GTPases. *J. Biol. Chem.* 274:13198–13204.

Bokoch, G.M., C.J. Vlahos, Y. Wang, U.G. Knaus, and A.E. Traynor-Kaplan. 1996. Rac GTPase interacts specifically with phosphatidylinositol 3-kinase. *Biochem. J.* 315:775–779.

Boveris, A., N. Oshino, and B. Chance. 1972. The cellular production of hydrogen peroxide. *Biochem. J.* 128:617–630.

Cai, J., and D.P. Jones. 1998. Superoxide in apoptosis. Mitochondrial generation triggered by cytochrome c loss. *J. Biol. Chem.* 273:11401–11404.

Caron, E., and A. Hall. 1998. Identification of two distinct mechanisms of phagocytosis controlled by different Rho GTPases. *Science.* 282:1717–1721.

Carthy, C.M., D.J. Granville, H. Jiang, J.G. Levy, C.M. Rudin, C.B. Thompson, B.M. McManus, and D.W. Hunt. 1999. Early release of mitochondrial cytochrome c and expression of mitochondrial epitope 7A6 with a porphyrin-derived photosensitizer: Bcl-2 and Bcl-xL overexpression do not prevent early mitochondrial events but still depress caspase activity. *Lab. Invest.* 79:953–965.

Chandel, N.S., E. Maltepe, E. Goldwasser, C.E. Mathieu, M.C. Simon, and P.T. Schumacker. 1998. Mitochondrial reactive oxygen species trigger hypoxia-induced transcription. *Proc. Natl. Acad. Sci. USA.* 95:11715–11720.

Datta, S.R., A. Katsov, L. Hu, A. Petros, S.W. Fesik, M.B. Yaffe, and M.E. Greenberg. 2000. 14-3-3 proteins and survival kinases cooperate to inactivate BAD by BH3 domain phosphorylation. *Mol. Cell.* 6:41–51.

del Peso, L., M. Gonzalez-Garcia, C. Page, R. Herrera, and G. Nunez. 1997. Interleukin-3-induced phosphorylation of BAD through the protein kinase Akt. *Science.* 278:687–689.

Droge, W. 2002. Free radicals in the physiological control of cell function. *Physiol. Rev.* 82:47–95.

Duchen, M.R. 1999. Contributions of mitochondria to animal physiology: from homeostatic sensor to calcium signalling and cell death. *J. Physiol.* 516:1–17.

Embade, N., P.F. Valeron, S. Aznar, E. Lopez-Collazo, and J.C. Lacal. 2000. Apoptosis induced by Rac GTPase correlates with induction of FasL and ceramides production. *Mol. Biol. Cell.* 11:4347–4358.

Esteve, P., N. Embade, R. Perona, B. Jimenez, L. del Peso, J. Leon, M. Arends, T. Miki, and J.C. Lacal. 1998. Rho-regulated signals induce apoptosis in vitro and in vivo by a p53-independent, but Bcl2 dependent pathway. *Oncogene.* 17:1855–1869.

Flohe, L., and F. Otting. 1984. Superoxide dismutase assays. *Methods Enzymol.* 105:93–104.

Forsayeth, J.R., and P.D. Garcia. 1994. Adenovirus-mediated transfection of cultured cells. *Biotechniques.* 17:354–356, 357–358.

Freeman, J.L., A. Abo, and J.D. Lambeth. 1996. Rac "insert region" is a novel effector region that is implicated in the activation of NADPH oxidase, but not PAK65. *J. Biol. Chem.* 271:19794–19801.

Gilmore, A.P., A.D. Metcalfe, L.H. Romer, and C.H. Streuli. 2000. Integrin-mediated survival signals regulate the apoptotic function of Bax through its conformation and subcellular localization. *J. Cell Biol.* 149:431–446.

Goossens, V., J. Grooten, K. De Vos, and W. Fiers. 1995. Direct evidence for tumor necrosis factor-induced mitochondrial reactive oxygen intermediates and their involvement in cytotoxicity. *Proc. Natl. Acad. Sci. USA.* 92:8115–8119.

Gottlieb, E., M.G. Vander Heiden, and C.B. Thompson. 2000. Bcl-x(L) prevents the initial decrease in mitochondrial membrane potential and subsequent reactive oxygen species production during tumor necrosis factor alpha-induced apoptosis. *Mol. Cell. Biol.* 20:5680–5689.

Han, D.C., L.G. Rodriguez, and J.L. Guan. 2001. Identification of a novel interaction between integrin beta1 and 14-3-3beta. *Oncogene.* 20:346–357.

Hockenbery, D.M., Z.N. Oltvai, X.M. Yin, C.L. Milliman, and S.J. Korsmeyer. 1993. Bcl-2 functions in an antioxidant pathway to prevent apoptosis. *Cell.* 75:241–251.

Huang, P., L. Feng, E.A. Oldham, M.J. Keating, and W. Plunkett. 2000. Superoxide dismutase as a target for the selective killing of cancer cells. *Nature.* 407: 390–395.

Irani, K., Y. Xia, J.L. Zweier, S.J. Sollott, C.J. Der, E.R. Fearon, M. Sundaresan, T. Finkel, and P.J. Goldschmidt-Clermont. 1997. Mitogenic signaling mediated by oxidants in Ras-transformed fibroblasts. *Science.* 275:1649–1652.

Joneson, T., and D. Bar-Sagi. 1998. A Rac1 effector site controlling mitogenesis through superoxide production. *J. Biol. Chem.* 273:17991–17994.

Joneson, T., M. McDonough, D. Bar-Sagi, and L. Van Aelst. 1996. RAC regulation of actin polymerization and proliferation by a pathway distinct from Jun kinase. *Science.* 274:1374–1376 (erratum published 276:185).

Joyce, D., B. Bouzahzah, M. Fu, C. Albanese, M. D'Amico, J. Steer, J.U. Klein, R.J. Lee, J.E. Segall, J.K. Westwick, et al. 1999. Integration of Rac-dependent regulation of cyclin D1 transcription through a nuclear factor-kappaB-dependent pathway. *J. Biol. Chem.* 274:25245–25249.

Kane, D.J., T.A. Sarafian, R. Anton, H. Hahn, E.B. Gralla, J.S. Valentine, T. Ord, and D.E. Bredesen. 1993. Bcl-2 inhibition of neural death: decreased generation of reactive oxygen species. *Science.* 262:1274–1277.

Kheradmand, F., E. Werner, P. Tremble, M. Symons, and Z. Werb. 1998. Role of Rac1 and oxygen radicals in collagenase-1 expression induced by cell shape change. *Science.* 280:898–902.

Korshunov, S.S., V.P. Skulachev, and A.A. Starkov. 1997. High protonic potential actuates a mechanism of production of reactive oxygen species in mitochondria. *FEBS Lett.* 416:15–18.

Koya, R.C., H. Fujita, S. Shimizu, M. Ohtsu, M. Takimoto, Y. Tsujimoto, and N. Kuzumaki. 2000. Gelsolin inhibits apoptosis by blocking mitochondrial membrane potential loss and cytochrome c release. *J. Biol. Chem.* 275: 15343–15349.

Kroemer, G., and J.C. Reed. 2000. Mitochondrial control of cell death. *Nat. Med.* 6:513–519.

Kusano, H., S. Shimizu, R.C. Koya, H. Fujita, S. Kamada, N. Kuzumaki, and Y. Tsujimoto. 2000. Human gelsolin prevents apoptosis by inhibiting apoptotic mitochondrial changes via closing VDAC. *Oncogene.* 19:4807–4814.

Lamarche, N., N. Tapon, L. Stowers, P.D. Burbelo, P. Aspenstrom, T. Bridges, J. Chant, and A. Hall. 1996. Rac and Cdc42 induce actin polymerization and G1 cell cycle progression independently of p65PAK and the JNK/SAPK MAP kinase cascade. *Cell.* 87:519–529.

Lee, A.C., B.E. Fenster, H. Ito, K. Takeda, N.S. Bae, T. Hirai, Z.X. Yu, V.J. Ferrans, B.H. Howard, and T. Finkel. 1999. Ras proteins induce senescence by altering the intracellular levels of reactive oxygen species. *J. Biol. Chem*. 274: 7936–7940.

Lee, S.R., K.S. Kwon, S.R. Kim, and S.G. Rhee. 1998. Reversible inactivation of protein-tyrosine phosphatase 1B in A431 cells stimulated with epidermal growth factor. *J. Biol. Chem.* 273:15366–15372.

Li, N., T.D. Oberley, L.W. Oberley, and W. Zhong. 1998. Inhibition of cell growth in NIH/3T3 fibroblasts by overexpression of manganese superoxide dismutase: mechanistic studies. *J. Cell. Physiol.* 175:359–369.

Madesh, M., and G. Hajnoczky. 2001. VDAC-dependent permeabilization of the outer mitochondrial membrane by superoxide induces rapid and massive cytochrome c release. *J. Cell Biol.* 155:1003–1015.

Manna, S.K., H.J. Zhang, T. Yan, L.W. Oberley, and B.B. Aggarwal. 1998. Overexpression of manganese superoxide dismutase suppresses tumor necrosis factor-induced apoptosis and activation of nuclear transcription factor-kappaB and activated protein-1. *J. Biol. Chem.* 273:13245–13254.

Marzo, I., C. Brenner, N. Zamzami, S.A. Susin, G. Beutner, D. Brdiczka, R. Remy, Z.H. Xie, J.C. Reed, and G. Kroemer. 1998. The permeability transition pore complex: a target for apoptosis regulation by caspases and bcl-2-related proteins. *J. Exp. Med.* 187:1261–1271.

McKay, N.D., B. Robinson, R. Brodie, and N. Rooke-Allen. 1983. Glucose transport and metabolism in cultured human skin fibroblasts. *Biochim. Biophys. Acta.* 762:198–204.

Nemoto, S., K. Takeda, Z.X. Yu, V.J. Ferrans, and T. Finkel. 2000. Role for mitochondrial oxidants as regulators of cellular metabolism. *Mol. Cell Biol*. 20: 7311–7318.

Nicholls, D.G., and S.L. Budd. 2000. Mitochondria and neuronal survival. *Physiol. Rev.* 80:315–360.

Nobes, C.D., and A. Hall. 1995. Rho, rac, and cdc42 GTPases regulate the assembly of multimolecular focal complexes associated with actin stress fibers, lamellipodia, and filopodia. *Cell.* 81:53–62.

Ozaki, M., S.S. Deshpande, P. Angkeow, S. Suzuki, and K. Irani. 2000. Rac1 regulates stress-induced, redox-dependent heat shock factor activation. *J. Biol. Chem*. 275: 35377–35383.

Page, K., J. Li, J.A. Hodge, P.T. Liu, T.L. Vanden Hoek, L.B. Becker, R.G. Pestell, M.R. Rosner, and M.B. Hershenson. 1999. Characterization of a Rac1 signaling pathway to cyclin D(1) expression in airway smooth muscle cells. *J. Biol. Chem.* 274:22065–22071.

Powers, S.K., F.K. Lieu, D. Criswell, and S. Dodd. 1993. Biochemical verification of quantitative histochemical analysis of succinate dehydrogenase activity in skeletal muscle fibres. *Histochem. J.* 25:491–496.

Qiu, R.G., J. Chen, D. Kirn, F. McCormick, and M. Symons. 1995. An essential role for Rac in Ras transformation. *Nature.* 374:457–459.

Racker, E. 1983. The Warburg effect: two years later. *Science.* 222:232.

Rook, G.A., J. Steele, S. Umar, and H.M. Dockrell. 1985. A simple method for the solubilisation of reduced NBT, and its use as a colorimetric assay for activation of human macrophages by gamma-interferon. *J. Immunol. Methods.* 82: 161–167.

Ruoslahti, E., and J.C. Reed. 1994. Anchorage dependence, integrins, and apoptosis. *Cell.* 77:477–478.

Sanchez-Alcazar, J.A., E. Schneider, M.A. Martinez, P. Carmona, I. Hernandez-Munoz, E. Siles, P. De La Torre, J. Ruiz-Cabello, I. Garcia, and J.A. Solis-Herruzo. 2000. Tumor necrosis factor-alpha increases the steady-state reduction of cytochrome b of the mitochondrial respiratory chain in metabolically inhibited L929 cells. *J. Biol. Chem.* 275:13353–13361.

Schindler, U., and V.R. Baichwal. 1994. Three NF-kappa B binding sites in the human E-selectin gene required for maximal tumor necrosis factor alpha-induced expression. *Mol. Cell. Biol.* 14:5820–5831.

Schulze-Osthoff, K., R. Beyaert, V. Vandevoorde, G. Haegeman, and W. Fiers. 1993. Depletion of the mitochondrial electron transport abrogates the cytotoxic and gene-inductive effects of TNF. *EMBO J.* 12:3095–3104.

Seto, M., U. Jaeger, R.D. Hockett, W. Graninger, S. Bennett, P. Goldman, and S.J. Korsmeyer. 1988. Alternative promoters and exons, somatic mutation and deregulation of the Bcl-2-Ig fusion gene in lymphoma. *EMBO J.* 7:123–131.

Shimizu, S., Y. Eguchi, W. Kamiike, Y. Funahashi, A. Mignon, V. Lacronique, H. Matsuda, and Y. Tsujimoto. 1998. Bcl-2 prevents apoptotic mitochondrial dysfunction by regulating proton flux. *Proc. Natl. Acad. Sci. USA.* 95:1455–1459.

Smiley, S.T., M. Reers, C. Mottola-Hartshorn, M. Lin, A. Chen, T.W. Smith, G.D. Steele, Jr., and L.B. Chen. 1991. Intracellular heterogeneity in mitochondrial membrane potentials revealed by a J-aggregate-forming lipophilic cation JC-1. *Proc. Natl. Acad. Sci. USA*. 88:3671–3675.

Smith, J., E. Ladi, M. Mayer-Proschel, and M. Noble. 2000. Redox state is a central modulator of the balance between self-renewal and differentiation in a dividing glial precursor cell. *Proc. Natl. Acad. Sci. USA.* 97:10032–10037.

Strasser, A., L. O'Connor, and V.M. Dixit. 2000. Apoptosis signaling. *Annu. Rev. Biochem.* 69:217–245.

Sudo, T., and M. Karin. 2000. Assays for JNK and p38 mitogen-activated protein kinases. *Methods Enzymol.* 322:388–392.

Suh, Y.A., R.S. Arnold, B. Lassegue, J. Shi, X. Xu, D. Sorescu, A.B. Chung, K.K. Griendling, and J.D. Lambeth. 1999. Cell transformation by the superoxide-generating oxidase Mox1. *Nature.* 401:79–82.

Sundaresan, M., Z.X. Yu, V.J. Ferrans, K. Irani, and T. Finkel. 1995. Requirement for generation of H2O2 for platelet-derived growth factor signal transduction. *Science*. 270:296–299.

Suzukawa, K., K. Miura, J. Mitsushita, J. Resau, K. Hirose, R. Crystal, and T. Kamata. 2000. Nerve growth factor-induced neuronal differentiation requires generation of Rac1-regulated reactive oxygen species. *J. Biol. Chem.* 275: 13175–13178.

Thannickal, V.J., and B.L. Fanburg. 2000. Reactive oxygen species in cell signaling. *Am. J. Physiol. Lung Cell. Mol. Physiol*. 279:L1005–L1028.

Tremble, P., R. Chiquet-Ehrismann, and Z. Werb. 1994. The extracellular matrix ligands fibronectin and tenascin collaborate in regulating collagenase gene expression in fibroblasts. *Mol. Biol. Cell.* 5:439–453.

Turrens, J.F., A. Alexandre, and A.L. Lehninger. 1985. Ubisemiquinone is the electron donor for superoxide formation by complex III of heart mitochondria. *Arch. Biochem. Biophys.* 237:408–414.

Vanden Hoek, T.L., Z. Shao, C. Li, P.T. Schumacker, and L.B. Becker. 1997. Mitochondrial electron transport can become a significant source of oxidative injury in cardiomyocytes. *J. Mol. Cell. Cardiol.* 29:2441–2450.

Vander Heiden, M.G., N.S. Chandel, X.X. Li, P.T. Schumacker, M. Colombini, and C.B. Thompson. 2000. Outer mitochondrial membrane permeability can regulate coupled respiration and cell survival. *Proc. Natl. Acad. Sci. USA.* 97:4666–4671.

Vander Heiden, M.G., N.S. Chandel, P.T. Schumacker, and C.B. Thompson. 1999. Bcl-xL prevents cell death following growth factor withdrawal by facilitating mitochondrial ATP/ADP exchange. *Mol. Cell.* 3:159–167.

Werner, E., F. Kheradmand, R. Isberg, and Z. Werb. 2001. Phagocytosis mediated by Yersinia invasin induces collagenase-1 expression in rabbit synovial fibroblasts through a pro-inflammatory cascade. *J. Cell Sci*. 114:3333–3343.

Westwick, J.K., Q.T. Lambert, G.J. Clark, M. Symons, L. Van Aelst, R.G. Pestell, and C.J. Der. 1997. Rac regulation of transformation, gene expression, and actin organization by multiple, PAK-independent pathways. *Mol. Cell. Biol.* 17:1324–1335.

Witke, W., A.H. Sharpe, J.H. Hartwig, T. Azuma, T.P. Stossel, and D.J. Kwiatkowski. 1995. Hemostatic, inflammatory, and fibroblast responses are blunted in mice lacking gelsolin. *Cell.* 81:41–51.

Woo, C.H., Y.W. Eom, M.H. Yoo, H.J. You, H.J. Han, W.K. Song, Y.J. Yoo, J.S. Chun, and J.H. Kim. 2000. Tumor necrosis factor-α generates reactive oxygen species via a cytosolic phospholipase A2-linked cascade. *J. Biol. Chem.* 275:32357–32362.

Yang, J., X. Liu, K. Bhalla, C.N. Kim, A.M. Ibrado, J. Cai, T.I. Peng, D.P. Jones, and X. Wang. 1997. Prevention of apoptosis by Bcl-2: release of cytochrome c from mitochondria blocked. *Science.* 275:1129–1132.

Zhai, J., H. Lin, M. Shamim, W.W. Schlaepfer, and R. Canete-Soler. 2001. Identification of a novel interaction of 14-3-3 with p190RhoGEF. *J. Biol. Chem.* 276:41318–41324.

Zhou, Y.P., J.C. Pena, M.W. Roe, A. Mittal, M. Levisetti, A.C. Baldwin, W. Pugh, D. Ostrega, N. Ahmed, V.P. Bindokas, et al. 2000. Overexpression of Bcl-x(L) in beta-cells prevents cell death but impairs mitochondrial signal for insulin secretion. *Am. J. Physiol. Endocrinol. Metab.* 278:E340–E351.

Zoratti, M., and I. Szabo. 1995. The mitochondrial permeability transition. *Biochim. Biophys. Acta.* 1241:139–176.